Chromatin motion is constrained by association with nuclear compartments in human cells

Current Biology, Vol. 12, 439–445, March 19, 2002, ©2002 Elsevier Science Ltd. All rights reserved. PII S0960-9822(02)00695-4

Chromatin Motion Is Constrained by Association with Nuclear Compartments in Human Cells

Jonathan R. Chubb, Shelagh Boyle, Paul Perry, and Wendy A. Bickmore[1]
MRC Human Genetics Unit
Western General Hospital
Crewe Road
Edinburgh, EH4 2XU
Scotland
United Kingdom

Summary

Background: In comparison with many nuclear proteins, the movement of chromatin in nuclei appears to be generally constrained. These restrictions on motion are proposed to reflect the attachment of chromatin to immobile nuclear substructures.

Results: To gain insight into the regulation of chromosome dynamics by nuclear architecture, we have followed the movements of different sites in the human genome in living cells. Here, we show that loci at nucleoli or the nuclear periphery are significantly less mobile than other, more nucleoplasmic loci. Disruption of nucleoli increases the mobility of nucleolar-associated loci.

Conclusions: This is the first report of distinct nuclear substructures constraining the movements of chromatin. These constraints reflect the physical attachment of chromatin to nuclear compartments or steric impairment caused by local ultrastructure. Our data suggest a role for the nucleolus and nuclear periphery in maintaining the three-dimensional organization of chromatin in the human nucleus.

Background

Studies of chromosome organization in interphase nuclei reveal a highly defined three-dimensional architecture. Individual chromosomes occupy discrete, nonoverlapping territories, and different genomic regions reproducibly localize to specific subnuclear positions. It is becoming clear that nuclear position may be a critical determinant of gene regulation. A nuclear peripheral localization, for example, has been correlated with transcriptionally silent chromatin in several experimental systems [1, 2].

The apparent reproducibility of chromatin organization likely depends upon the relative immobility of chromatin during interphase. Two complementary experimental approaches have confirmed that the motion of interphase chromatin is generally constrained. Fluorescence recovery after photobleaching (FRAP) studies on mammalian nuclei indicate that chromatin is immobile over distance scales greater than 0.4 μm, for time periods of more than 1 hr [3]. This contrasts with other FRAP experiments indicating that many nuclear proteins are able to diffuse across an entire nucleus in less than a minute [4]. The restrictions on chromatin motion can also be demonstrated at the single-molecule level by following individual fluorescently tagged loci. Tracking the movements of a single pericentromeric locus in budding yeast revealed that chromatin is able to undergo substantial diffusional mobility. However, consistent with the FRAP studies, this motion was confined to a region with an approximate radius of 0.25 μm [5].

The confinement of chromatin observed in these studies has implications for our understanding of nuclear structure. One view suggests that the restrictions to chromatin motion may simply reflect steric interactions between large and possibly highly entangled DNA polymers. Diffusion of DNA molecules in solution is several orders of magnitude more rapid than the observed diffusion in FRAP experiments [3], and many studies indicate that chromosomes are not extensively intermingled in interphase nuclei [6]. Together, these observations suggest that steric interactions between chromosomes alone may not account for the observed constraints on chromatin motion. An alternative view it that the restrictions on chromatin motion reflect the attachment of chromatin to nuclear substructures, such as the nucleolus, nuclear periphery, or a global superstructure such as a nuclear matrix [7]. An extension of this model suggests that, by varying the density of attachment sites, the mobility of chromatin can be tightly regulated, which may account for large-scale movements of chromatin observed in specific developmental and tissue culture models [8].

To gain insight into the regulation of chromatin dynamics by nuclear architecture, we have analyzed the motion of several different regions in the human genome. The genomic regions we have studied differ in terms of gene density, replication timing, intranuclear position, and association with nuclear compartments. The movements of these different loci were therefore expected to reveal the different forces governing chromatin mobility. This is the first study to compare the mobility of different loci in mammalian cells and to address the impact of nuclear compartments on chromatin dynamics. We show that chromatin associated with the nucleolus or nuclear periphery is more restricted in its movements than other, more nucleoplasmic, genomic regions. Our data likely reflect the physical attachment of chromatin to nuclear compartments, or steric impairment to motion caused by local ultrastructure, and may reflect a role for the nucleolus and nuclear periphery in maintaining the organization of chromatin in the nucleus.

Results

Tagging Different Sites in the Human Genome

To monitor chromatin movements in living human cells, we tagged individual loci with arrays of lacO sequences [9]. GFP was directed to these arrays by fusing it to the

[1]Correspondence: w.bickmore@hgu.mrc.ac.uk

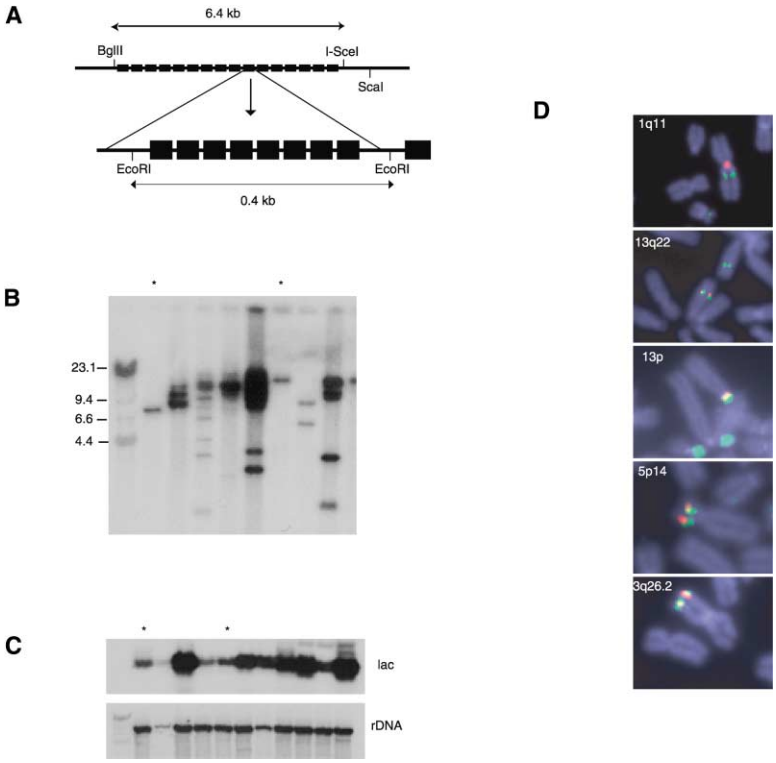

Figure 1. Tagging Different Regions of the Human Genome with lacO Arrays

(A) A schematic of the 128-mer lacO array.

(B) A Southern blot of BglII-digested genomic DNA from lac integrant cells hybridized to a lac probe. Single-copy clones are marked with an asterisk.

(C) Southern blots of EcoRI-digested genomic DNA from lac integrant cells hybridized to lac and rDNA probes. The band intensity relative to single-copy clones was used to determine the lac copy number for all cell lines.

(D) Integration of lacO arrays into different genomic regions determined by FISH with a lac probe (red). Integration sites confirmed using probes derived from BAC clones from the same or adjacent chromosome bands (green). The 13p integration is compared to an rDNA probe.

lac repressor, allowing the tagged loci to be visualized as fluorescent spots. We integrated a 128-mer array (Figure 1A) of lacO sequences randomly into the genome of HT-1080 cells [10]. The array copy number in each of the clones was determined using Southern hybridization of genomic DNA digested with BglII, which has a unique site in the lacO array vector. We found two independent clones that give single bands of between 7.4 kb and 14.8 kb, indicating that these clones have single-copy insertions of the array, not multiple, inverted repeat, or fragmented insertions (Figure 1B). These single-copy clones were used to estimate the array copy number of the other clones (Figure 1C). The smallest integrations used previously in mammalian cells were 10–20 copies of a 256-mer lac array [11]. Here, we have used 7–16 copies of a 128-mer array. Fluorescence in situ hybridization (FISH) of metaphase spreads using a lac probe indicated that, in each of these positive clones, the lac arrays had integrated at a single locus (Figure 1D). The cytogenetic position of these loci was determined and confirmed using probes known to hybridize to particular bands (Figure 1D). Five cell lines were chosen as the basis for this study. The genomic regions tagged in these clones have different properties in terms of gene density, replication timing, intranuclear position, and association with nuclear compartments [12] (Table 1).

It was important to determine if the integration of lacO sequences perturbed intranuclear chromosome organization. FISH with probes to lacO and the genomic regions of integration was used to compare the positions of tagged and untagged loci in the same cells. The lac arrays have similar intranuclear distributions to their untagged homologs (Figures 2A and 2B) and reflect the known distributions of human chromosomes [2]. The array integrated at 13p, close to rDNA, is always found at the nucleolus (33/33 nuclei, Figure 2B). The 1q11 array is found in the nuclear interior (Figure 2A). 1q11 is a satellite-rich region known to associate with nucleoli [13]. Consistent with this, 92% (54/59) of spots in the 1q11 cells expressing GFP-repressor overlap with Ki67 antigen staining (data not shown). The 13q22 array is enriched at the nuclear periphery. The arrays at 5p14 and 3q26.2 show less polarized distributions, with 5p14 distributed throughout the nucleus and 3q26.2 enriched close to, but not at, the nuclear periphery. In all of our cell lines, no significant recruitment of GFP-repressor spots to promyelocytic leukemia (PML) bodies was seen. This contrasts with an earlier study demonstrating the recruitment of megabase-sized operator arrays to PML bodies [14] (Figure 2C).

Chromatin Motion Constrained at Nuclear Compartments

Chromatin motion was tracked in the lacO integrant cell lines stably expressing the GFP-lac repressor fusion protein. We followed the movements of the tagged loci by observing the changes in distance between two GFP-lac spots [5]. Approximately 30% of the cells had two spots, corresponding to two copies of the integrated chromosome, as HT-1080 cells display aneuploidy [15].

The movement of individual loci in human cells is restricted, as demonstrated in the time lapse of a single nucleus in Figure 3A. The changes in distance between spots, from several different nuclei of the 5p14 integrant, are illustrated in Figure 3B. These data support the idea of the random walk diffusive behavior inferred from studies on yeast chromatin [5]. For many of the data records, the distance between spots appears to fluctuate, apparently randomly, around a mean value. For other records, there appears to be a more substantial drift away from

Table 1. Properties of lacO Array-Tagged Loci

Integration Site	Array Copy Number	Genomic Region	Subnuclear Localization
13q22	7	R band	Peripheral
5p14	12	G band	Nucleoplasmic
3q26.2	10	R band	Nucleoplasmic
13p	7	Close to rDNA	Nucleolar
1q11	16	Satellite	Nucleolar

G bands contain AT-rich, late-replicating, and relatively gene-poor DNA. R bands, in contrast, contain GC-rich, early-replicating, and gene-dense DNA that is packaged with hyperacetylated histones [12, 17].

the initial position, with some records showing movements of over a micron. The magnitude of the change in distance between two spots is independent of the distance between the two spots (Figure 3B).

For freely diffusing particles, the mean square displacement (MSD) from the origin varies linearly with time [16]. We refer to the mean square change in distance ($<\Delta d^2>$), which is proportional to the MSD and does not require a fixed origin [8]. A plot of $<\Delta d^2>$ against time for the 5p14 locus shows clear linearity, indicating diffusive motion (Figure 3C). The gradient of this line reflects the diffusion coefficient for the 5p14 locus. This was found to be 1.25×10^{-4} $\mu m^2/s$, approximately 4-fold lower than the coefficient estimated for budding yeast [5], indicating that human chromatin experiences greater resistance to motion. The slope of the $<\Delta d^2>$ plot decays for the later time points, indicating that the diffusion of the 5p14 locus is constrained. The $<\Delta d^2>$ value at which the plot tails off reflects the degree of constraint on the locus. The asymptotic $<\Delta d^2>$ value of 0.22 μm^2 indicates a mean change in distance between spots of 0.48 μm. This value is 2-fold higher than the estimate from yeast, indicating that human chromatin has a greater radius of movement. A plot of $<\Delta d^2>$ for fixed 5p14 cells indicates that experimental noise caused by our equipment is minimal. The behavior of a second locus, at 3q26.2, is similar to 5p14 (Figure 3C). The two loci both have similar diffusion coefficients, and the asymptotic level of the 3q26.2 plot is not statistically different from that of the 5p14 plot. 5p14 and 3q26.2 are G and R bands, respectively, and their underlying DNA differs in its base composition, gene density, and replication timing. G bands contain AT-rich, late-replicating, and relatively gene-poor DNA. R bands, in contrast, contain GC-rich, gene-dense DNA that replicates early in S-phase [17]. It is therefore significant that chromatin mobility, which likely reflects the degree of attachment to nuclear substructures and local steric compaction, is similar in both chromosomal environments.

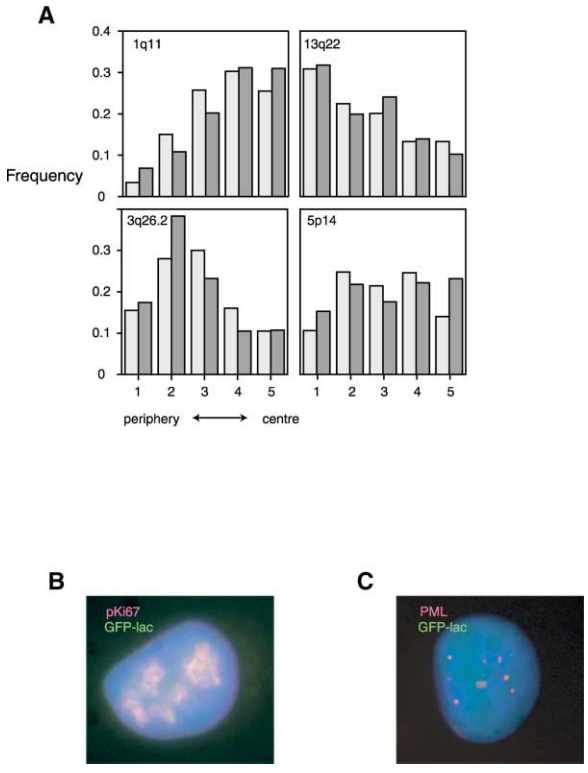

Figure 2. lacO Arrays Behave Like Endogenous Loci

(A) Different subnuclear distributions of tagged loci. A total of 100 nuclei per cell line were divided by erosion of segmented nuclei into 5 concentric shells [29]. Hybridization signals for lac (dark) and BAC (light) probes were assigned to the shells.

(B) The lacO array at 13p, close to rDNA, associates with the nucleolus.

(C) No significant recruitment of lac arrays to PML bodies.

We also obtained $<\Delta d^2>$ values from genomic regions located at or adjacent to the nucleolus and nuclear periphery. As can be seen from the plots in Figure 4A, peripheral and nucleolar-associated chromatin is considerably less mobile than the nucleoplasmic 5p14 locus. The $<\Delta d^2>$ plot for the nuclear peripheral 13q22 locus initially has a similar gradient to the two nucleoplasmic loci, but the asymptotic $<\Delta d^2>$ value indicates a mean change in distance between spots of 0.3 μm, significantly lower than the values obtained from the nucleoplasmic loci ($p = 0.0001$). The difference in the range of movement between 13q22 and 5p14 is clearly apparent in the untransformed data (Figure 4B). The maximum range of movement for 13q22 was 0.9 μm, compared to the 1.5 μm observed for the 5p14 locus. In general, the displacements observed for 5p14 were greater. Nucleolar-associated chromatin also displays impeded motion. The $<\Delta d^2>$ plots for the 13p and 1q11 loci have much lower trajectories than those for the nucleoplasmic loci, indicating that they are more constrained.

Mobility of Nucleolar Chromatin after Nucleolar Disruption

To assess the importance of nucleolar ultrastructure in the constraints on chromatin motion, we treated the 13p integrant cell line with the transcriptional inhibitor 5,6-dichloro-D-ribofuranosylbenzimidazole (DRB). After

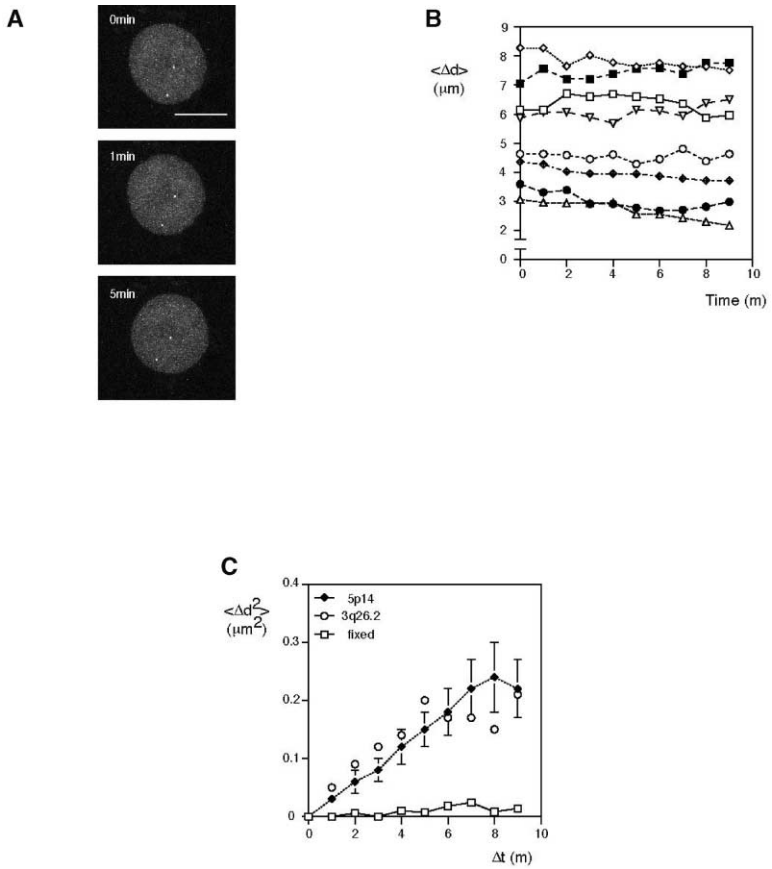

Figure 3. Movements of Individual Loci in Human Cells

(A) Time lapse of a 5p14 integrant cell stably expressing GFP-lac repressor; the scale bar represents 10 μm.

(B) Changes in distance (<Δd>) between GFP spots over time for several different 5p14 nuclei.

(C) A plot of $<\Delta d^2>$ against time for the 5p14 (filled diamonds), 3q26.2 (circles), and fixed 5p14 (squares) nuclei. The standard error for the 5p14 locus is shown (n = 46 nuclei).

treatment of human fibroblasts with DRB, nucleolar structure is disrupted (Figure 5A) and the rDNA and satellite sequences that comprise the DNA component of the nucleolus disperse through the nuclear interior [18]. Treatment of the 13p integrant cells with DRB significantly increases the mobility of the tagged locus compared to untreated cells (Figure 5B, $p = 0.0058$). When DRB was removed and fresh medium was added to the culture, we observed a decrease in the mobility of the 13p locus (Figure 5B), which parallels the reemergence of prominent nucleoli in many cells. If the increased level of motion induced by DRB was a consequence of the global lack of RNA polymerase II activity, we would expect nonnucleolar chromatin to also become more mobile upon DRB treatment. This is not the case (Figure 5C). Treatment of the 13q22 integrant cells with DRB clearly has no effect on the mobility of this peripheral locus, indicating that the constraints on the movement of 13p are likely to be imposed by nucleolar architecture.

Discussion

This is the first study to describe movements of individual loci in human cells. The chromatin mobility we have described is broadly similar to the diffusional mobility identified in other systems, but we have shown that different loci display different levels of motion. Genomic regions associated with the nucleolus and nuclear periphery display significantly more constrained movements than other, more nucleoplasmic loci. In the case of nucleolar-associated loci, this restriction on motion can be alleviated by the pharmacological disruption of the nucleolus. Our data demonstrate that nuclear compartments such as the nucleolus and nuclear periphery constrain chromatin motion.

Although the lacO system is becoming a widely used experimental tool in studies on the biology of the nucleus [19], previous studies have not addressed the level of disruption of chromosomal architecture caused by the integration of the lacO arrays. The insertion of 2 Mb of repetitive sequence at the *Drosophila brown* locus results in the association of the locus with centromeric heterochromatin [20]. A consequence of somatic pairing of homologous chromosomes in *Drosophila* is that the wild-type *brown* allele is also recruited to heterochromatin. The resulting transcriptional silencing gives rise to a dominant variegating phenotype. In addition, previous studies on chromosome motion in mammalian cells using the lacO system have used large arrays of operators that localize at the nuclear periphery [14, 21, 22]. Although our lacO integrations are smaller than any used previously in mammalian cells, we were initially concerned that these arrays might have disruptive effects on chromosome organization and cause recruitment of the tagged loci to silent nuclear domains. However, our FISH studies demonstrate that the lac arrays have subnuclear distributions appropriate for their sites of integration and also show appropriate recruitment to both

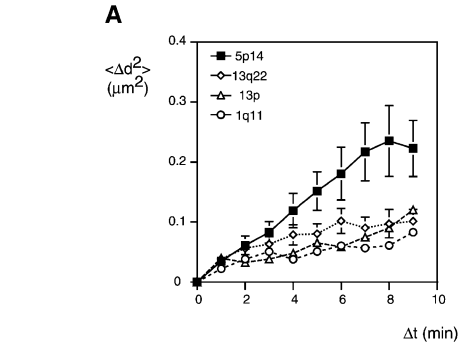

Figure 4. Reduced Mobility of Chromatin at the Nucleolus and Nuclear Periphery

(A) $<\Delta d^2>$ plots for 13p (triangles), 1q11 (circles), and 13q22 (diamonds) loci. For comparison, the 5p14 plot is also shown (filled symbols). The nucleolar (1q11 and 13p) and nuclear peripheral (13q22) loci are clearly less mobile than the nucleoplasmic loci. The standard error is shown for the 13q22 locus (n = 47).

(B) Raw $<\Delta d>$ values for 5p14 and 13q22 loci. All time points for all nuclei are included.

nucleoli and the nuclear periphery. We did not find significant enrichment of the arrays at PML bodies, in contrast to an earlier study [14]. Our arrays were over two orders of magnitude smaller than those used previously, which may account for the differences between the data.

Our chromatin motion data suggest broad similarities in the motile properties of interphase chromatin from budding yeast, *Drosophila*, and humans. Quantitative analysis of the mobility of human chromatin is suggestive of motion by diffusion, as reported for other organisms. Our data also suggest that this diffusion is constrained, and we show that the level of constraint varies between loci. Although superficially similar, the properties of the constrained diffusional motion we see in human cells are quantitatively different from those of the other model organisms. We estimate the diffusion coefficients for human loci to be 4-fold lower than the coefficient estimated from budding yeast [5], implying that human chromatin is subject to greater resistance to motion. This may reflect that mammalian chromatin shows a greater degree of compaction or is more extensively attached to nuclear substructures. The constraints on motion also differ between species. The asymptotic mean change in distance for the 5p14 locus is over 2-fold higher than the estimate from yeast, indicating that human chromatin has a greater radius of movement. However, due to the large size of the human nucleus, loci are constrained to a much smaller proportion of the total nuclear volume than in yeast. A recent chromatin motion study in *Drosophila* spermatocytes reveals multiple levels of constraint [8]. Over time intervals of a few seconds, the chromatin is restricted to submicron-sized regions of the nucleus. Over time periods of an hour or more, individual loci are considerably more mobile and appear to have access to regions several microns in diameter. Although we did not address large-scale chro-

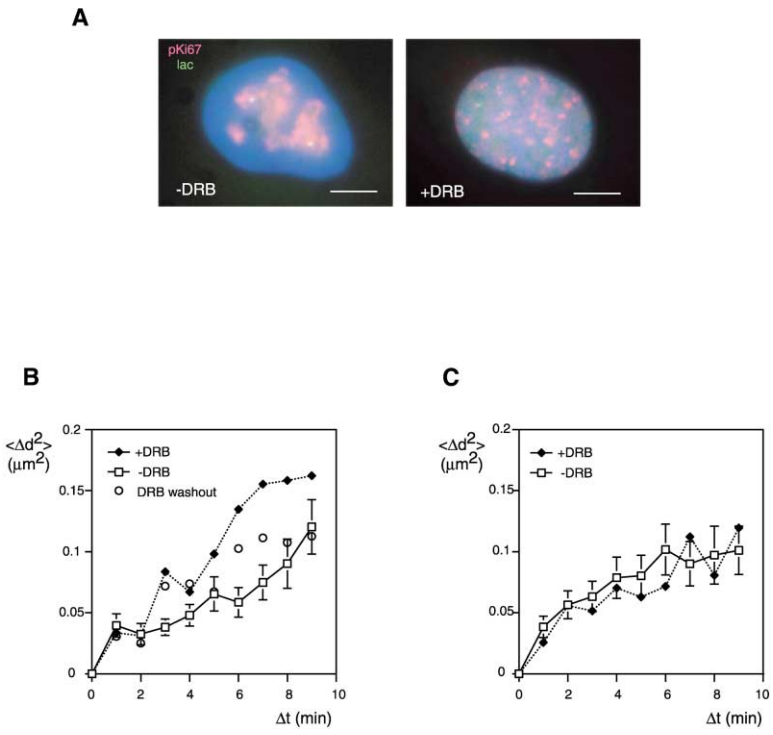

Figure 5. Constraints on Chromatin Motion Imposed by Nucleolar Ultrastructure

(A) Nucleolar dispersal mediated by DRB. 13p integrant cells stained with anti-pKi67 (red) after 5 hr in the presence or absence of 50 μg/ml DRB. 13p loci tagged with a GFP-repressor are shown in green; the scale bars represent 5 μm.

(B) Enhanced mobility of the 13p locus induced by DRB. The washout experiment was carried out 18 hr after DRB-containing medium was replaced by fresh medium, by which time prominent nucleoli had reformed in many cells.

(C) DRB does not affect the mobility of the nuclear peripheral 13q22 locus.

matin movement in this study, FRAP experiments indicate that chromatin in HeLa cells is restricted to submicron-sized regions, even over observation periods of an hour [3]. This indicates that the long-range movement observed in *Drosophila* spermatocytes may not be a property of human chromatin. Analysis of the motion of different loci in a number of different cell types will be required to assess how general the parameters we have calculated are for human chromatin. Progression through the cell cycle is also likely to be an important determinant of chromatin mobility. The long-range motion of *Drosophila* chromatin is apparent in spermatocytes in early G2; however, these large movements subside later in G2 as the cells approach meiotic prophase. Furthermore, a recent yeast study indicates that the diffusive movement of chromatin observed in G1 becomes more constrained during S-phase [23].

We have analyzed the effects of nuclear substructures on chromosome dynamics and have shown that proximity to the nucleolus and nuclear periphery can constrain chromatin motion. Nucleolar dispersal reduces the constraint on the motion of nucleolar-associated chromatin, indicating that compartment ultrastructure is required for restriction of motion. The linear ranges of movement differ by 1.5- to 2-fold between nucleoplasmic and compartment-associated loci. However, in terms of the nuclear volume that chromatin has access to, compartment-associated loci are restricted to a region 4–8 times smaller than nucleoplasmic loci. These constraints could conceivably result from steric impairment to chromatin motion imposed by the ultrastructure of these compartments. The nuclear periphery, for example, has been correlated with transcriptionally silent, late-replicating chromatin in several model systems [1, 2, 24]. The greater restriction to chromatin movements at the nuclear periphery may therefore result from a more condensed, heterochromatic environment.

An alternative view suggests that constraints on chromatin motion result from the physical attachment of chromatin to nuclear structures such as the nuclear lamina, nucleolus, or a nuclear matrix. This model, first suggested by Abney et al. (1997) was proposed to account for the chromatin immobility they inferred from FRAP studies. An extension of this model suggests that, by regulating the density of attachment sites, chromatin dynamics can be tightly controlled [8]. Our data provide strong experimental support for these physical attachment models and indicate that the nuclear periphery and nucleolus are likely nuclear substrates for the attachment of chromatin. Telomeric DNA is associated with nuclear pore complexes in budding yeast [25], demonstrating that direct physical attachment of chromatin to the nuclear periphery can occur. We have also shown that the mobility of chromatin not associated with the nucleolus or nuclear periphery is less constrained. This implies that the attachments of chromatin to the nucleolus and nuclear periphery are likely to have a more profound effect on the regulation of chromatin dynamics than interactions with any global superstructure such as a nuclear matrix. This may reflect a role for these compartments in maintaining the three-dimensional organization of chromatin in the nucleus.

Experimental Procedures

Generation of lacO Integrant Cell Lines

An EcoRI fragment containing an 8-mer array of lacO sites was released from pSV2-DHFR-8.32 [9] and cloned into pBluescript (Stratagene). The 8-mer was then cloned using BamHI and SalI into pUC21 [26]. The array was doubled in size, with BglII/NotI fragments carrying the 8-mer recloned back into the original vector linearized with BamHI/NotI. The amplification process was repeated, yielding a 128-mer lacO array. Cloning operations were carried out in recombination-deficient STBL2 *Escherichia coli* (Invitrogen). The 128-mer vector was linearized with ScaI and cotransfected with the selection vector pSV2-bsr into HT-1080 cells using Lipofectamine 2000 (Invitrogen). Selection was carried out in DMEM supplemented with 10% fetal calf serum in the presence of 5 μg/ml blasticidinS. Colonies were picked after 10 days of selection and grown until sufficient cells were available for Southern blotting [27], freezing, and FISH. Southerns were hybridized to α-^{32}P-labeled probes labeled from the 8-mer EcoRI fragment of pUC21-128lac and the 7.1-kb EcoRI fragment of pHSR-7.1 [28] (rDNA). For expression of the GFP-lac protein in these lacO cell lines, we utilized the p3′SS-GFP-lac-NLS vector [9]. Stable cell lines expressing GFP-repressor were selected using 100 μg/ml hygromycin.

Fluorescence In Situ Hybridization and Immunofluorescence

FISH on methanol/acetic acid-fixed nuclei and chromosomes was carried out essentially as described [29]. The rDNA and lac probes were generated by nick translation of pHSR-7.1 [28] and 128-mer lac vector, respectively. BAC probes, 105-E-14 (1q12), 5-N-11 (5p13.3-14), 31-C-06 (13q22), and 151-P-12 (3q26.2), were obtained from BACPAC. Erosion scripts [29], run by IPLab software, were used to quantify the intranuclear distributions of the FISH signals. A total of 100 nuclei were studied for each cell line. To identify PML bodies or the nucleolar antigen pKi67, immunofluorescence was carried out on cells fixed with 4% paraformaldehyde and permeabilized with 0.2% Triton X-100. Mouse 5E10 (anti-PML [30]) or rabbit anti-human Ki67 (DAKO) antibodies were applied, both diluted ten fold in PBS. After application of Texas red-conjugated secondary antibodies (Vector), the cells were washed in PBS, then mounted in 1 μg/ml 4,6-diamidino-2-phenylindole (DAPI) in Vectashield (Vector). The results from both immunofluorescence and FISH experiments were viewed on a Zeiss Axioplan fluorescence microscope. Quantification of the colocalization of GFP-lac spots with nuclear bodies was performed by multitracking confocal microscopy on a Zeiss LSM510.

Visualization of Chromatin Motion in Live HT-1080 Cells

Live cell analysis was performed using the Bioptechs Delta T open dish system (Bioptechs), mounted on the stage of the Zeiss LSM510 confocal microscope. The cells were cultured to 80% confluency for the experiments in medium buffered by the addition of 25 mM HEPES (pH 7). Under these conditions, the culture retains a normal frequency of dividing cells for the time period of image capture. The LSM510 was run using the FITC capture parameters of the Zeiss LSM510 software version 2.8. A single 30-frame z stack, with a 0.5 μm z interval was collected every minute, for 10 min, with a scan time of 1.5 s. To exclude error in measurement caused by *z* axis resolution and nuclear rotation, we selected nuclei in which the two spots remained on the same confocal z section (Figure 2A), an approach used previously in studies on budding yeast and *Drosophila* nuclei [8, 23]. Distances were calculated in two rather than in three dimensions, a process expected to cause a slight underestimate in our values for chromatin confinement radii, as *z* axis displacements are not taken into account. In two dimensions, distances are calculated using $d = \sqrt{(x^2 + y^2)}$. In three dimensions, distances should be calculated using $d = \sqrt{(x^2 + y^2 + z^2)}$. A basic property of diffusive behavior is that a random walk is unbiased, so we expect an equal probability of motion along all axes. Therefore, the ratio of d_{3D} to d_{2D} is $\sqrt{(3x^2/2x^2)}$ which equals $\sqrt{(3/2)}$ or 1.22. Multiplying our two-dimensional estimates for confinement radii by this scalar does not affect any of our conclusions. The position of a GFP-lac spot was defined as the brightest pixel. The change in distance between the spots relative to $t = 0$ ($<\Delta d>$) was calculated for each data record

at each time point. The Δd values were squared, and a mean value of the squared change was calculated for each time point ($<\Delta d^2>$). Standard normal deviates were calculated from the last four time points to assess the significance of the apparent differences between $<\Delta d^2>$ values. We estimated the diffusion coefficient, D, from the slopes of $<\Delta d^2>$ plots. The gradient of a $<\Delta d^2>$ plot for a particle undergoing a two-dimensional random walk is equal to 4D [16].

Acknowledgments

J.R.C. is in receipt of a Medical Research Council Research Training Fellowship, and W.A.B. is a James S. McDonnell Centennial Fellow. We thank Andrew Belmont for the pSV2-DHFR-8.32 and p3′SS-GFP-lac-NLS vectors, Andrew Carothers for help with statistical analysis of the data, and Nick Hastie and Peter Currie for comments on the manuscript.

Received: November 27, 2001
Revised: January 11, 2002
Accepted: January 14, 2002
Published: March 19, 2002

References

1. Andrulis, E.D., Neiman, A.M., Zappulla, D.C., and Sternglanz, R. (1998). Perinuclear localization of chromatin facilitates transcriptional silencing. Nature *394*, 592–595.
2. Boyle, S., Gilchrist, S., Bridger, J.M., Mahy, N.L., Ellis, J.A., and Bickmore, W.A. (2001). The spatial organization of human chromosomes within the nuclei of normal and emerin-mutant cells. Hum. Mol. Genet. *10*, 211–219.
3. Abney, J.R., Cutler, B., Fillbach, M.L., Axelrod, D., and Scalettar, B.A. (1997). Chromatin dynamics in interphase nuclei and its implications for nuclear structure. J. Cell Biol. *137*, 1459–1468.
4. Phair, R.D., and Misteli, T. (2000). High mobility of proteins in the mammalian cell nucleus. Nature *404*, 604–609.
5. Marshall, W.F., Straight, A., Marko, J.F., Swedlow, J., Dernburg, A., Belmont, A., Murray, A.W., Agard, D.A., and Sedat, J.W. (1997). Interphase chromosomes undergo constrained diffusional motion in living cells. Curr. Biol. *7*, 930–939.
6. Cremer, T., and Cremer, C. (2001). Chromosome territories, nuclear architecture and gene regulation in mammalian cells. Nat. Rev. Genet. *2*, 292–301.
7. Zink, D., and Cremer, T. (1998). Cell nucleus: chromosome dynamics in nuclei of living cells. Curr. Biol. *8*, R321–R324.
8. Vazquez, J., Belmont, A.S., and Sedat, J.W. (2001). Multiple regimes of constrained chromosome motion are regulated in the interphase *Drosophila* nucleus. Curr. Biol. *11*, 1227–1239.
9. Robinett, C.C., Straight, A., Li, G., Willhelm, C., Sudlow, G., Murray, A., and Belmont, A.S. (1996). In vivo localization of DNA sequences and visualization of large-scale chromatin organization using lac operator/repressor recognition. J. Cell Biol. *135*, 1685–1700.
10. Rasheed, S., Nelson-Rees, W.A., Toth, E.M., Arnstein, P., and Gardner, M.B. (1974). Characterization of a newly derived human sarcoma cell line (HT-1080). Cancer *33*, 1027–1033.
11. Tumbar, T., and Belmont, A.S. (2001). Interphase movements of a DNA chromosome region modulated by VP16 transcriptional activator. Nat. Cell Biol. *3*, 134–139.
12. Bridger, J.M., and Bickmore, W.A. (1998). Putting the genome on the map. Trends Genet. *14*, 403–409.
13. Stahl, A., Hartung, M., Vagner-Capodano, A.M., and Fouet, C. (1976). Chromosomal constitution of nucleolus-associated chromatin in man. Hum. Genet. *35*, 27–34.
14. Tsukamoto, T., Hashiguchi, N., Janicki, S.M., Tumbar, T., Belmont, A.S., and Spector, D.L. (2000). Visualization of gene activity in living cells. Nat. Cell Biol. *2*, 871–878.
15. Itzhaki, J.E., Barnett, M.A., MacCarthy, A.B., Buckle, V.J., Brown, W.R., and Porter, A.C. (1992). Targeted breakage of a human chromosome mediated by cloned human telomeric DNA. Nat. Genet. *2*, 283–287.
16. Berg, H.C. (1983). Random Walks in Biology (Princeton, NJ: Princeton University Press).
17. Craig, J.M., and Bickmore, W.A. (1993). Chromosome bands—flavours to savour. Bioessays *15*, 349–354.
18. Haaf, T., and Ward, D.C. (1996). Inhibition of RNA polymerase II transcription causes chromatin decondensation, loss of nucleolar structure, and dispersion of chromosomal domains. Exp. Cell Res. *224*, 163–173.
19. Belmont, A.S. (2001). Visualizing chromosome dynamics with GFP. Trends Cell Biol. *11*, 250–257.
20. Csink, A.K., and Henikoff, S. (1996). Genetic modification of heterochromatic association and nuclear organization in *Drosophila*. Nature *381*, 529–531.
21. Li, G., Sudlow, G., and Belmont, A.S. (1998). Interphase cell cycle dynamics of a late-replicating, heterochromatic homogeneously staining region: precise choreography of condensation/decondensation and nuclear positioning. J. Cell Biol. *140*, 975–989.
22. Tumbar, T., and Belmont, A.S. (2001). Interphase movements of a DNA chromosome region modulated by VP16 transcriptional activator. Nat. Cell Biol. *3*, 134–139.
23. Heun, P., Laroche, T., Shimada, K., Furrer, P., and Gasser, S.M. (2001). Chromosome dynamics in the yeast interphase nucleus. Science *294*, 2181–2186.
24. Heun, P., Laroche, T., Raghuraman, M.K., and Gasser, S.M. (2001). The positioning and dynamics of origins of replication in the budding yeast nucleus. J. Cell Biol. *152*, 385–400.
25. Galy, V., Olivo-Marin, J.C., Scherthan, H., Doye, V., Rascalou, N., and Nehrbass, U. (2000). Nuclear pore complexes in the organization of silent telomeric chromatin. Nature *403*, 108–112.
26. Vieira, J., and Messing, J. (1991). New pUC-derived cloning vectors with different selectable markers and DNA replication origins. Gene *100*, 189–194.
27. Church, G.M., and Gilbert, W. (1984). Genomic sequencing. Proc. Natl. Acad. Sci. USA *81*, 1991–1995.
28. Yoon, Y., Sanchez, J.A., Brun, C., and Huberman, J.A. (1995). Mapping of replication initiation sites in human ribosomal DNA by nascent-strand abundance analysis. Mol. Cell. Biol. *15*, 2482–2489.
29. Croft, J.A., Bridger, J.M., Boyle, S., Perry, P., Teague, P., and Bickmore, W.A. (1999). Differences in the localization and morphology of chromosomes in the human nucleus. J. Cell Biol. *145*, 1119–1131.
30. Stuurman, N., de Graaf, A., Floore, A., Josso, A., Humbel, B., de Jong, L., and van Driel, R. (1992). A monoclonal antibody recognizing nuclear matrix-associated nuclear bodies. J. Cell Sci. *101*, 773–784.